THE JOURNAL OF PHYSICAL CHEMISTRY C

ARTICLE

pubs.acs.org/JPCC

Prediction of Silicon Nanowires as Photocatalysts for Water Splitting: Band Structures Calculated Using Density Functional Theory

R.Q. Zhang,[†] X.M. Liu,[‡] Z. Wen,[†] and Q. Jiang[†,*]

[†]Key Laboratory of Automobile Materials (Jilin University), Ministry of Education, and School of Materials Science and Engineering, Jilin University, Changchun, 130022, China

[‡]College of Chemistry, Jilin University, Changchun, 130012, China

ABSTRACT: Hydrogen as an efficient energy carrier is an environmentally benign fuel of the future. Solar-powered water splitting, using semiconductor photocatalysts, is an efficient generation method of hydrogen where excellent photocatalysts are key factors. In this work, we investigate silicon nanowires (SiNWs) as photocatalysts for the water splitting. By utilizing density functional theory calculations, we demonstrated that SiNWs terminated with suitable H and Cl surface coverage should be a promising photocatalyst for this purpose. The interaction between Cl-3*p* and surface Si-3*p* states of SiNWs leads to suitable reducing and oxidizing powers simultaneously while the separation of HOMO and LUMO of SiNWs prevents the electron−hole recombination.

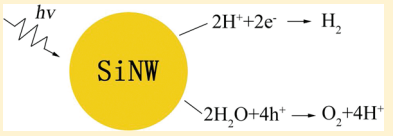

INTRODUCTION

It is an ultimate goal to produce hydrogen from water using solar energy for the supply of clean and recyclable energy. Considerable attention has been drawn in recent years to develop semiconductors that exhibit excellent photocatalytic properties.[1−3] A number of photocatalysts have been proposed, and some have achieved high quantum efficiencies. The process of water splitting by solar energy, which utilizes both reducing and oxidation powers of semiconductor photocatalysts, is shown in part a of Figure 1, where E_1 and E_2 denote the reducing and oxidizing potentials of water redox, respectively. The reducing and oxidizing powers are measured by the energy of the conduction band minimum (CBM) E_{CBM} and the valence band maximum (VBM) E_{VBM}, respectively. $\Delta_1 = E_{CBM} - E_1$ and $\Delta_2 = E_2 - E_{VBM}$ are defined. The larger Δ_1 (Δ_2), the stronger the reducing (oxidizing) power is. For a spontaneous water splitting process, the oxygen and hydrogen reactions must lie between the CBM and VBM, that is the band edges of semiconductor photocatalysts must straddle the water redox potential levels. However, it is well-known that the band gap (E_g) of a desirable semiconductor photocatalyst should be around 2.0 eV to effectively utilize solar energy. Therefore, a semiconductor photocatalyst must meet two requirements: band edges straddling the water redox potential levels and E_g = ∼2.0 eV.

Recently, there are many reports about the excellent optical properties of silicon nanowires (SiNWs) and their application in the solar cell.[4−7] These results encourage us to investigate the potential of SiNWs as photocatalysts for water splitting. As is well known, bulk Si is unsuitable for photocatalysts due to the narrow and indirect E_g, especially the high E_{VBM} compared with the oxidizing potential of water redox.[1] Fortunately, SiNWs have a wider band gap due to the quantum confinement effect, as concluded by both the first principle calculations[8,9] and the experiment results.[10] Simultaneously, an indirect-to-direct band-gap transition occurs in SiNWs with diameters of several nanometers and SiNWs exhibit advantageous optical properties.[11,12] It is reported that H-terminated SiNWs were employed as photocatalysts in the degradation of rhodamine B, as well as oxidization of benzyl alcohol to benzoic acid.[13] However, SiNWs as a photocatalyst for the water splitting has not yet been reported. In this contribution, using DFT, we investigate the photocatalysis of

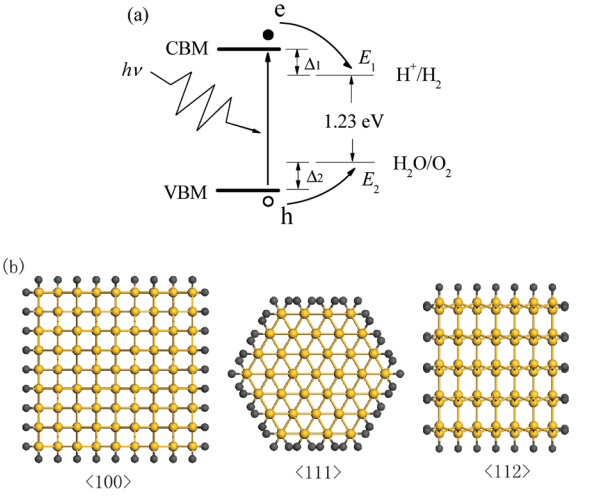

Figure 1. (a) Schematic diagram for the principle of water splitting by semiconductor photocatalysts using solar energy. **e** and **h** denote electron and hole respectively. $E_1 - E_2$ = 1.23 eV. (b) Top view of the ball and stick structures of ⟨100⟩, ⟨111⟩, and ⟨112⟩ SiNWs with *D* of 2.0, 1.5, and 1.7 nm, respectively. *D* is defined as that of the circular shape with same area of the nanowire. The big and small balls denote Si and the terminating groups.

Received: November 23, 2010
Revised: January 2, 2011
Published: February 03, 2011

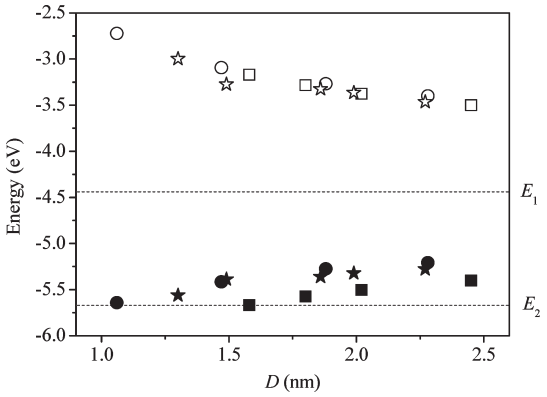

Figure 2. E_{VBM} (filled) and E_{CBM} (unfilled) of ⟨100⟩ (square), ⟨111⟩ (circle), and ⟨112⟩ (star) H-terminated SiNWs with different D. The dot lines are standard water redox potentials E_1 and E_2. The reference potential is the vacuum level.

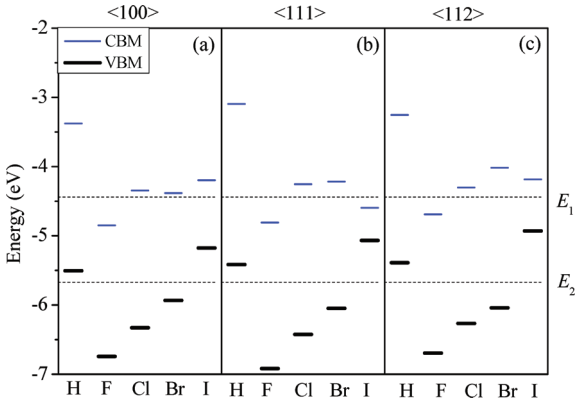

Figure 3. Site levels of VBM and CBM for (a) ⟨100⟩, (b) ⟨111⟩, and (c) ⟨112⟩ SiNWs terminated with halogen elements compared with H-terminated SiNWs. The dot lines are standard water redox potentials E_1 and E_2. The reference potential is the vacuum level.

SiNWs and demonstrate that SiNWs satisfy the both requirements by choosing suitable surface-terminating groups.

COMPUTATIONAL METHODS

The calculations are carried out by using DFT,[14,15] which is implemented in the DMol3 module.[16,17] The generalized gradient approximation (GGA) functional with the HCTH method,[18] being a nonlocal functional, is used as the exchange-correlation functional. All Electron Relativistic,[19] which includes all core electrons explicitly and introduces some relativistic effects into the core, is utilized for the core treatment. In addition, Double Numerical plus polarization[16] is chosen as the basis set with orbital cutoff of 4.6 Å. We use smearing techniques[20] with a smearing value of 0.005 Ha (1 Ha = 27.2114 eV). The structure of SiNWs is then relaxed by using the delocalized internal coordinate optimization scheme. The convergence tolerance of energy is 1.0×10^{-5} Ha, maximum force is 0.002 Ha/Å, and maximum displacement is 0.005 Å in the geometry optimization.

The structures of ⟨100⟩, ⟨111⟩, and ⟨112⟩ SiNWs with the diameter D of 2.0, 1.5, and 1.7 nm respectively are shown in part b of Figure 1. The cross sections of ⟨100⟩, ⟨111⟩, and ⟨112⟩ SiNWs are square, regular hexagon, and rectangle, respectively. ⟨100⟩ and ⟨111⟩ SiNWs are enclosed by (110) facets, whereas ⟨112⟩ SiNWs are enclosed by (110) and (111) facets. The stoichiometry of ⟨100⟩, ⟨111⟩, and ⟨112⟩ SiNWs are $Si_{81}M_{36}$, $Si_{74}M_{42}$, and $Si_{70}M_{34}$ in the unit cell respectively, where M denotes the terminating groups. The model possesses the local structure of bulk Si. The SiNW is placed in unit cell where the distance of interwires is larger than 12 Å, which effectively prevents the interaction effect from neighboring cells.

RESULTS AND DISCUSSION

H atoms are usually utilized to saturate the surface dangling bond of SiNWs in experiments.[10] Figure 2 shows the energy of VBM and CBM of H-terminated ⟨100⟩, ⟨111⟩, and ⟨112⟩ SiNWs with different D. Although the water redox potential levels are related to the pH value of an aqueous solution, we here only consider the situation of using standard water redox potentials (i.e., $E_1 = -4.44$ eV and $E_2 = -5.67$ eV) for references.[21,22] The requirement of $E_g = \sim 2.0$ eV can be satisfied at $D = 1.5-2.5$ nm. However, $E_{VBM} > E_2$, or the hole cannot spontaneously transfer to the oxidizing potential of the water splitting. Although its reducing power is strong ($E_{CBM} > E_1$), the band edges of H-terminated SiNWs cannot satisfy the requirement of straddling the water redox potential levels and H-terminated SiNWs are unsuitable as photocatalysts for this purpose. Therefore, it is necessary to find the strategy for drop of E_{VBM}.

It is reported that surface-terminated groups of halogen elements can be utilized to modulate the electronic band structures of SiNWs.[23] H atoms thus were replaced with halogen elements. We calculated three structures of ⟨100⟩, ⟨111⟩, and ⟨112⟩ SiNWs with terminating groups and different D of 2.0, 1.5, and 1.7 nm. First, we investigated the situation of all H atoms replaced by halogen elements (F, Cl, Br, I). Figure 3 shows the site levels of VBM and CBM of ⟨100⟩, ⟨111⟩, and ⟨112⟩ SiNWs terminated with H and halogen elements, which are compared with the water redox potential levels E_1 and E_2. As a whole, SiNWs with different growth directions have similar results for the same terminating group. Therefore, the effect of terminating groups on E_g is independent of growth directions. For the simplicity of discussion, we concentrate on the ⟨100⟩ $Si_{81}M_{36}$ nanowire (NW) in the following. As forementioned in Figure 2, $Si_{81}H_{36}$ NW is unsuitable for the photocatalysis. When all H atoms were replaced with halogen atoms, E_{CBM} and E_{VBM} of $Si_{81}F_{36}$, $Si_{81}Cl_{36}$, $Si_{81}Br_{36}$ NWs decrease, whereas E_{VBM} of $Si_{81}I_{36}$ NW increases and E_{CBM} of $Si_{81}I_{36}$ NW decreases compared with that of $Si_{81}H_{36}$ NW. E_{CBM} of $Si_{81}F_{36}$ NW drops down too much that the electron cannot spontaneously transfer to the reducing potential of the water splitting. E_g of $Si_{81}Cl_{36}$ NW straddles the water redox potential levels with the magnitude of about 2.0 eV, as shown in part a of Figure 3. Although the band edges of $Si_{81}Br_{36}$ NW straddle the water redox potential levels, $E_g = 1.5$ eV. In addition, $Si_{81}I_{36}$ NW cannot meet the both requirements of photocatalysts for the water splitting. Thus, $Si_{81}Cl_{36}$ NW has the best electronic band structure among these NWs. However, as displayed in part a of Figure 3, small Δ_1 value of 0.09 eV of $Si_{81}Cl_{36}$ NW implies a weak reducing power and a low reaction rate of reducing reaction. It is known that the reaction rate is related with the concentration of reactants and rate constants. In our case, the former may be considered as a constant during the reaction because the incident light induces the same quantity of electrons and holes where the oxidizing supplies H^+ for the reducing. According to the Arrhenius equation, $k = Ae^{-E_a/RT}$ where k denotes the rate constant of a chemical reaction with the activation energy E_a at a temperature T, A is the prefactor, and R

dx.doi.org/10.1021/jp111182c |J. Phys. Chem. C 2011, 115, 3425–3428

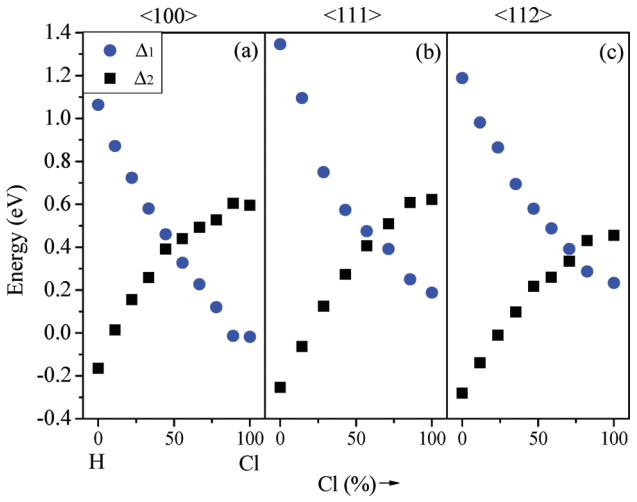

Figure 4. Phase diagram of Δ_1 and Δ_2 for (a) ⟨100⟩, (b) ⟨111⟩, and (c) ⟨112⟩ SiNWs with progressive surface coverage of H and Cl-terminating groups.

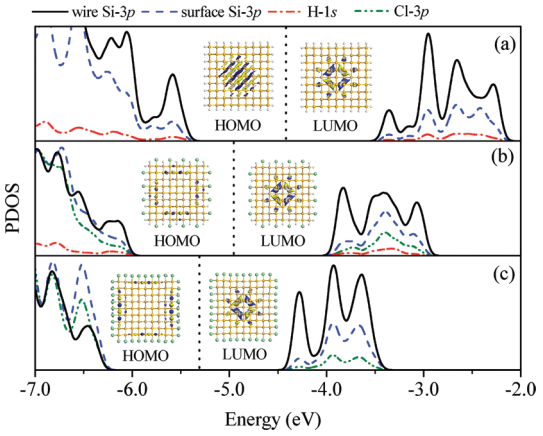

Figure 5. PDOS of core Si 3p (solid line) and surface Si 3p (dash line), H 1s (dash dot line), Cl 3p (dash dot dot line) orbitals per atom for ⟨100⟩ (a) $Si_{81}H_{36}$, (b) $Si_{81}H_{20}Cl_{16}$, and (c) $Si_{81}Cl_{36}$ NWs. The insert is the distribution of HOMO and LUMO. The legends are shown in the top. The dot lines are Fermi level. The reference potential is the vacuum level.

is the gas constant. The efficiency of the water splitting is maximized when the both processes of oxidizing and reducing reactions have the same reaction rate. Because A, T, and R in the above equation are the same, the unique decisive factor is the E_a value. In this reaction, the reducing power Δ_1 and the oxidizing power Δ_2 represent E_a values. Thus, the condition with the maximized efficiency is $\Delta_1 = \Delta_2$.

It is reported that Cl substituting H atoms on the surface of SiNWs gradually affect electronic band structures.[23] We thus consider the effect of different surface coverages of Cl atoms to obtain advisible reducing and oxidizing powers simultaneously. Figure 4 displays phase diagram of Δ_1 and Δ_2 as functions of Cl surface coverage (Cl%). It is found that for all three ⟨100⟩, ⟨111⟩, and ⟨112⟩ SiNWs, Δ_1 decreases, whereas Δ_2 increases, as Cl% increases. Although E_g of SiNWs decreases from 2.1 to 2.0 eV for ⟨100⟩ SiNWs as Cl% increases from 0 to 100%,[23] E_g values of partial Cl-terminated SiNWs always satisfy the requirement of E_g = ∼2.0 eV. H-terminated SiNWs have the largest Δ_1 or E_{a1}, whereas Cl-terminated SiNWs have the largest Δ_2 or E_{a2}, which is confirmed in Figure 3. Indeed, we can get a suitable point where $E_{a1} = E_{a2}$, as shown in Figure 4. For ⟨100⟩, ⟨111⟩, and ⟨112⟩ SiNWs, the corresponding Cl% values are 44.4% ($Si_{81}H_{20}Cl_{16}$ NW), 57.1% ($Si_{74}H_{18}Cl_{24}$ NW), and 70.6% ($Si_{70}H_{10}Cl_{24}$ NW), respectively.

Lastly, the atomic decomposed partial density of states (PDOS) is used to analyze the physical mechanism for modulating of different terminating groups on the electric band structures of SiNWs. Figure 5 shows the results of ⟨100⟩ SiNWs as a reference (SiNWs with other growth directions have similar phenomena). Si atoms in SiNWs are divided into two parts of surface Si atoms (bonding with terminating groups) and core Si atoms (all others). Similar to literature results,[24] the band edges are determined by the core Si atoms, whereas H atoms don't introduce additional energy bands there, as shown in part a of Figure 5. This is because H−Si bonding is stronger than Si−Si bonding, which pulls the surface states out of the band gap and into the conduction and valence bands. For $Si_{81}Cl_{36}$ NW, there is a significant weight of surface Si 3p states contributing to the valence band edge due to the hybridization of Cl 3p and surface Si 3p states. This result is consistent with the case of VBM and CBM changes of 3 nm thick Si−Cl slab due to the same hybridization.[23] Thus, the band energy and Fermi level of $Si_{81}Cl_{36}$ NW decrease, which is exhibited in part c of Figure 5 where PDOS shifts left, compared with that of $Si_{81}H_{36}$ NW. As results, E_{VBM} of $Si_{81}Cl_{36}$ NW decreases to satisfy the requirement of oxidizing process of the water splitting, as observed in Figure 3. Similar with $Si_{81}H_{36}$ NW, H 1s states do not contribute to the band edges of $Si_{81}H_{20}Cl_{16}$ NW. Surface Si 3p states of $Si_{81}H_{20}Cl_{16}$ NW contribute more to the valence band edges than that in $Si_{81}H_{36}$ NW due to the interaction of the hybridization of Cl 3p and surface Si 3p states. In summary, the partial replacing H with Cl brings out the suitable band edges energy of SiNWs, namely the mezzo reducing and oxidizing powers for water splitting.

It is known that the dominant loss mechanism of photocatalysts is the electron−hole recombination. Figure 5 show the distributions of highest occupied molecular orbital (HOMO) and lowest unoccupied molecular orbital (LUMO). It is interesting that the distribution of HOMO migrates to the surface with Cl% increasing, whereas LUMO always distributes in the center of SiNWs. The separation of HOMO and LUMO impedes the electron−hole recombination. This elevates the photocatalytic efficiency. This phenomenon is consistent with the enhancement of photocatalytic efficiency for degradation of rhodamine B by noble metal-modified SiNWs to separate electrons.[13]

Cl can substitute for H on Si surfaces and in porous Si through wet chemistry process,[25] whereas Cl surface coverage can be measured by using the frequencies of Si−H mode when the surfaces are commonly covered with H and Cl atoms.[26] Thus, this designed material can be obtained experimentally. In addition, because porous Si can be modeled as a collection of interacting NWs, the results obtained in this work can be extended to the porous Si. The advantages of using porous Si is that the chemistry is well known, it is highly photo stable, cheap and also nontoxic, as like as TiO_2 in water splitting.[3]

CONCLUSIONS

In light of DFT calculations, we have demonstrated that SiNWs with common surface coverage of H and Cl should be a promising photocatalyst for the water splitting by using solar energy. Coexistence of H and Cl atoms on the surfaces effectuates

SiNWs to present mezzo reducing and oxidizing powers simultaneously. It is found that the interaction between Cl 3p and surface Si 3p states brings out the drop of E_{VBM} of Cl-terminated SiNWs. Simultaneously, Cl atoms in the surface separate the distribution of HOMO and LUMO, which prevents the electron−hole recombination. The realization of SiNWs as photocatalyst for water splitting is thus hopeful.

AUTHOR INFORMATION

Corresponding Author
*Fax: 86-431-85095371, E-mail: jiangq@jlu.edu.cn.

ACKNOWLEDGMENT

We acknowledge support from the National Key Basic Research, Development Program (Grant No. 2010CB631001), from the Program for Changjiang Scholars and Innovative Research Team in University, and the High Performance Computing Center (HPCC) of Jilin University for supercomputer time.

REFERENCES

(1) Kudo, A.; Miseki, Y. *Chem. Soc. Rev.* **2009**, *38*, 253–278.
(2) Maeda, K.; Domen, K. *Chem. Mater.* **2009**, *22*, 612–623.
(3) Liu, M.; de Leon Snapp, N.; Park, H. *Chem. Sci.* **2011**, *2*, 80–87.
(4) Peng, K.; Wang, X.; Lee, S.-T. *Appl. Phys. Lett.* **2008**, *92*, 163103.
(5) Tian, B.; Kempa, T. J.; Lieber, C. M. *Chem. Soc. Rev.* **2009**, *38*, 16–24.
(6) Kelzenberg, M. D.; Boettcher, S. W.; Petykiewicz, J. A.; Turner-Evans, D. B.; Putnam, M. C.; Warren, E. L.; Spurgeon, J. M.; Briggs, R. M.; Lewis, N. S.; Atwater, H. A. *Nat. Mater.* **2010**, *9*, 239–244.
(7) Hochbaum, A. I.; Yang, P. *Chem. Rev.* **2009**, *110*, 527–546.
(8) Read, A. J.; Needs, R. J.; Nash, K. J.; Canham, L. T.; Calcott, P. D. J.; Qteish, A. *Phys. Rev. Lett.* **1992**, *69*, 1232.
(9) Zhao, X.; Wei, C. M.; Yang, L.; Chou, M. Y. *Phys. Rev. Lett.* **2004**, *92*, 236805.
(10) Ma, D. D. D.; Lee, C. S.; Au, F. C. K.; Tong, S. Y.; Lee, S. T. *Science* **2003**, *299*, 1874–1877.
(11) Buda, F.; Kohanoff, J.; Parrinello, M. *Phys. Rev. Lett.* **1992**, *69*, 1272.
(12) Li, J.; Freeman, A. J. *Phys. Rev. B* **2006**, *74*, 075333.
(13) Liu, Q.; Zhou, Y.; Kou, J.; Chen, X.; Tian, Z.; Gao, J.; Yan, S.; Zou, Z. *J. Am. Chem. Soc.* **2010**, *132*, 14385–14387.
(14) Hohenberg, P.; Kohn, W. *Phys. Rev.* **1964**, *136*, B864.
(15) Kohn, W.; Sham, L. J. *Phys. Rev.* **1965**, *140*, A1133.
(16) Delley, B. *J. Chem. Phys.* **1990**, *92*, 508–517.
(17) Delley, B. *J. Chem. Phys.* **2000**, *113*, 7756–7764.
(18) Boese, A. D.; Handy, N. C. *J. Chem. Phys.* **2001**, *114*, 5497–5503.
(19) Koelling, D. D.; Harmon, B. N. *J. Phys. C* **1977**, *10*, 3107–3114.
(20) Delley, B. DMol, a standard tool for density functional calculations: Review and advances. In *Theoretical and Computational Chemistry*; Seminario, J. M.; Politzer, P., Eds.; Elsevier: New York; Vol. 2, pp 221−254, 1995.
(21) Maier, F.; Riedel, M.; Mantel, B.; Ristein, J.; Ley, L. *Phys. Rev. Lett.* **2000**, *85*, 3472.
(22) Chakrapani, V.; Angus, J. C.; Anderson, A. B.; Wolter, S. D.; Stoner, B. R.; Sumanasekera, G. U. *Science* **2007**, *318*, 1424–1430.
(23) Leu, P. W.; Shan, B.; Cho, K. *Phys. Rev. B* **2006**, *73*, 195320.
(24) Aradi, B.; Ramos, L. E.; Deak, P.; Kohler, T.; Bechstedt, F.; Zhang, R. Q.; Frauenheim, T. *Phys. Rev. B* **2007**, *76*, 035305.
(25) Buriak, J. M. *Chem. Rev.* **2002**, *102*, 1271–1308.
(26) Ferguson, G. A.; Aureau, D.; Chabal, Y.; Raghavachari, K. *J. Phys. Chem. C* **2010**, *114*, 17644–17650.